

SUPPLEMENTARY FIGURE LEGENDS

Supplementary Fig. 1. Purification of autocatalytically processed Yca1. (A) Gel filtration profile of *E. coli*-expressed full-length wild-type Yca1. Purified Yca1 was eluted from Superdex-200 gel filtration column in a fraction corresponding to an apparent molecular mass of approximately 35 kDa. The eluted Yca1 protein contains two subunits comprising residues 1-331 and 335-432, respectively. (B) Autocatalytic processing occurs after Lys331 and Lys334 in Yca1. N-terminal peptide sequencing indicates that autoprocessing of Yca1 may occur at the carboxyl-end of Lys331 and Lys334. The blue and red arrows indicate possible autoprocessing sites.

Supplementary Fig. 2. Disruption of the homo-dimeric interface in canonical caspases by two extra β -strands of Yca1. (Left) Homo-dimer of caspase-3. Two molecules of caspase-3 form a homo-dimer (green & yellow) (PDB code 1CP3 (1)). (Top right) Structure of Yca1 monomer. The two extra β -strands of Yca1 (blue) that may disrupt canonical caspase-like homo-dimerization are encircled in red. (Bottom right) Structural alignment of Yca1 monomer to caspase-3 monomer. Structural alignment showed that the two extra β -strands of Yca1 (blue) induce steric clash with the adjacent caspase-3 molecule (yellow) during homo-dimer formation.

Supplementary Fig. 3. Structural comparison of the active sites of Yca1, caspase-3, caspase-9 and the paracaspase MALT1. (Left) Structural overlay of active sites of Yca1 and caspase-3. A close-up view on the Yca1 (blue) and caspase-3 (green) (PDB code 1CP3 (1)) active sites is shown. The covalently bound inhibitor Acetyl-Asp-Val-Ala-Asp-fluoromethyl ketone (Ac-DVAD-fmk) is highlighted in orange. (Middle) Structural overlay of Yca1 and caspase-9. A close-up view on the Yca1 (blue) and caspase-9 (magenta) (PDB code 1JXQ (2)) active sites is shown. The covalently bound inhibitor benzoxycarbonyl-Glu-Val-Asp-dichlorobenzylmethyl ketone (z-EVD-dcbmk) is highlighted in cyan. (Right) Structural overlay of Yca1 and MALT1. A close-up view on the Yca1 (blue) and MALT1 (yellow) (PDB code 3UOA (3)) active sites is shown. The covalently bound inhibitor benzoxycarbonyl-Val-Arg-Pro-Arg (z-VRPR-fmk) is highlighted in purple.

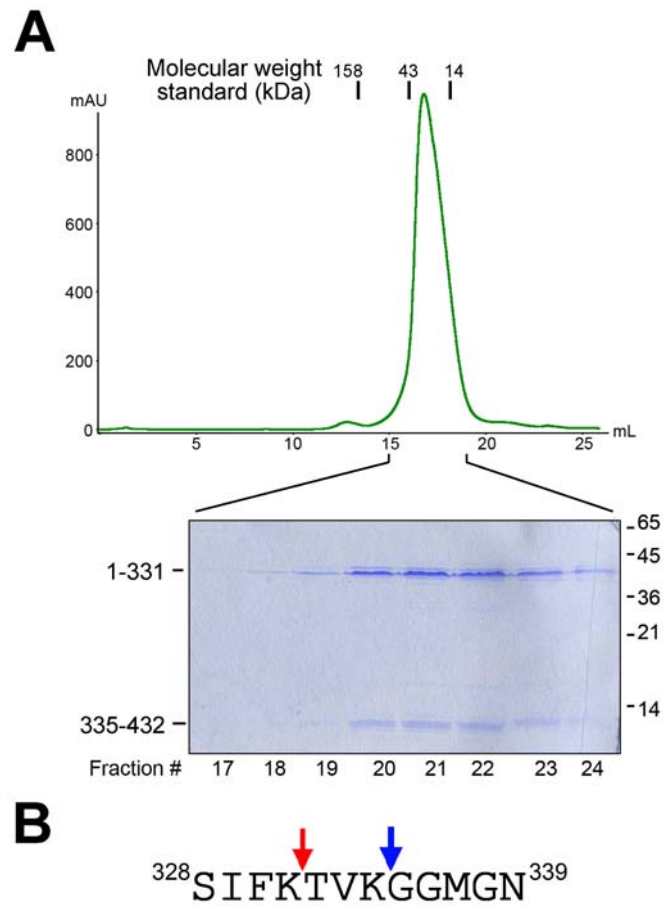
Supplementary Fig. 4. Identification of Ca^{2+} -stimulated, additional processing sites in autoprocessed Yca1. Single mutation of Arg72 or Lys86 reduced the 36-kDa doublet to a single band (lanes 2 & 3), whereas simultaneous mutation of Arg72 and Lys86 led to complete absence of the 36-kDa doublet in the presence of 10 mM Ca^{2+} (lane 4).

Supplementary Fig. 5. The N-terminal fragment of Yca1 does not affect its protease activity. To examine whether the N-terminal sequences of Yca1 inhibits its protease activity similarly as the case for MCA2 (4), we generated two variants: Yca1- Δ 86, which had the

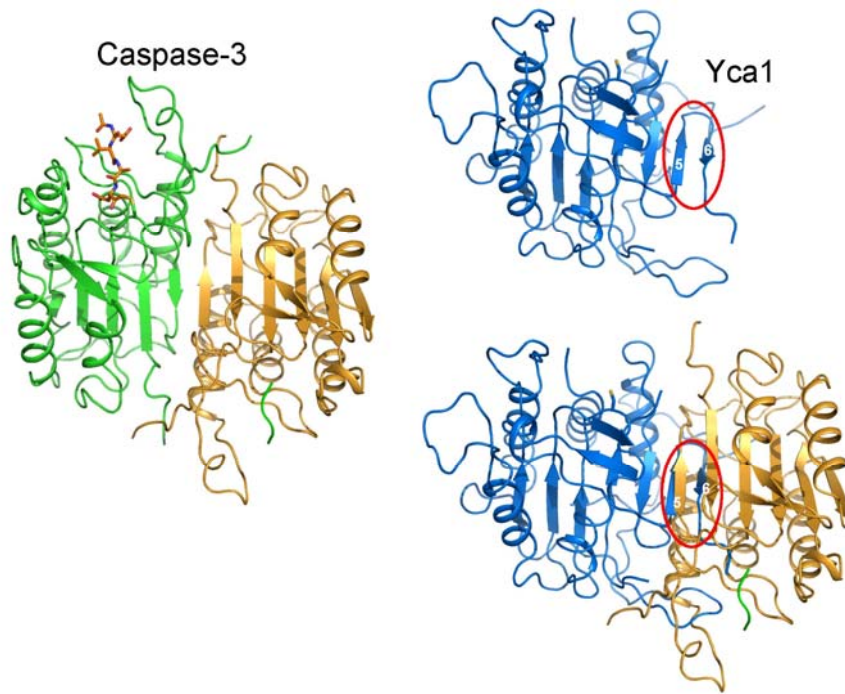
N-terminal 86 amino acids deleted, and Yca1-R72A/K86A. The protease activity assay, measured by the disappearance of the substrate Bir1 (residues 1-435), reveals that both Yca1- Δ 86 and Yca1-R72A/K86A exhibited a similar level of protease activity compared to the WT Yca1 protein. Note that the variant Yca1-R72A/K86A migrated a bit faster in the presence of Ca^{2+} on SDS-PAGE (lanes 3 & 4).

Supplementary Fig. 6. Autoprocessing of Yca1 can occur in *trans*. The presence of Ca^{2+} facilitated the auto-processing of MBP-Yca1 into a doublet of bands at about 60-kDa (lanes 1 & 2), which we believe represent MBP-Yca1(1-72/86). The presence of Ca^{2+} had no impact on the auto-catalytic processing of the mutant MBP-Yca1-C276A (lanes 7 & 8). Notably, in the presence of both Ca^{2+} and Yca1, the mutant MBP-Yca1-C276A was processed into the characteristic doublet of 60-kDa (lanes 5 & 6). This result indicates that auto-cleavage at R72/K86 can occur in *trans*, at least *in vitro* using purified recombinant proteins.

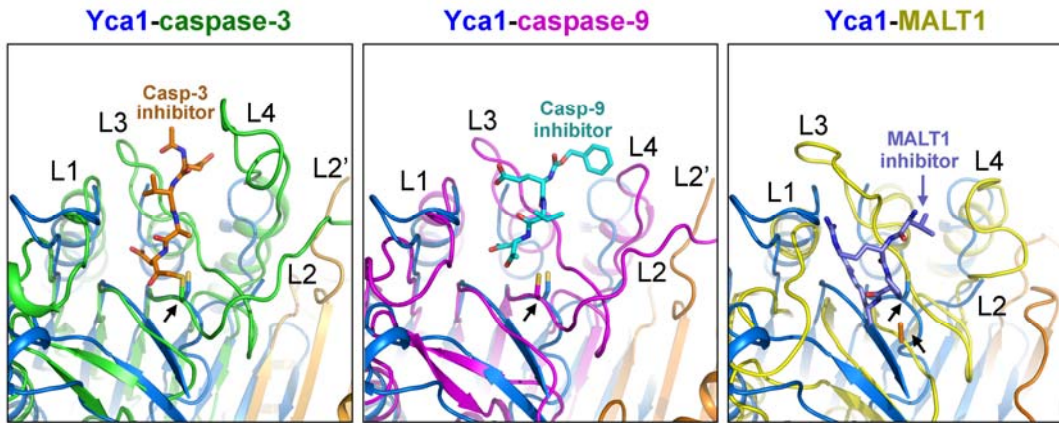
Supplementary Figure 1



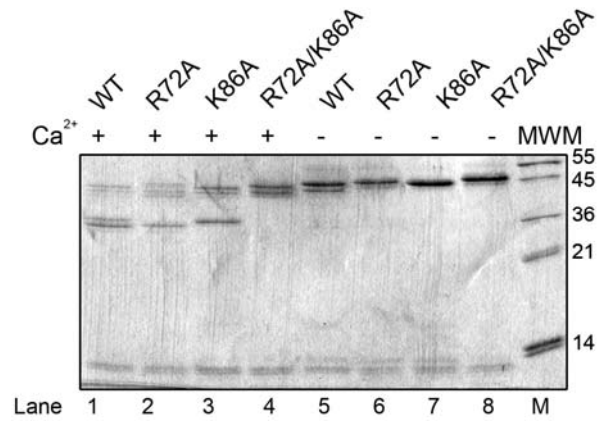
Supplementary Figure 2



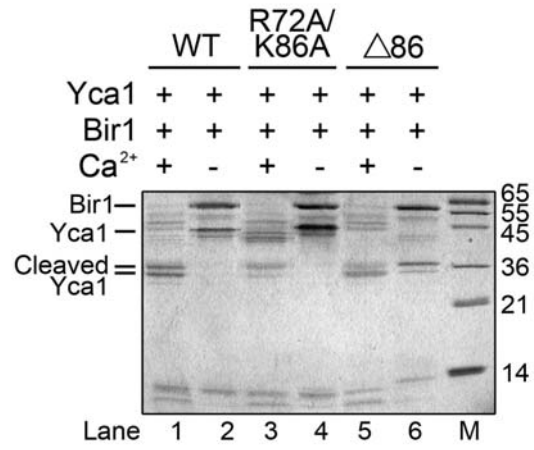
Supplementary Figure 3



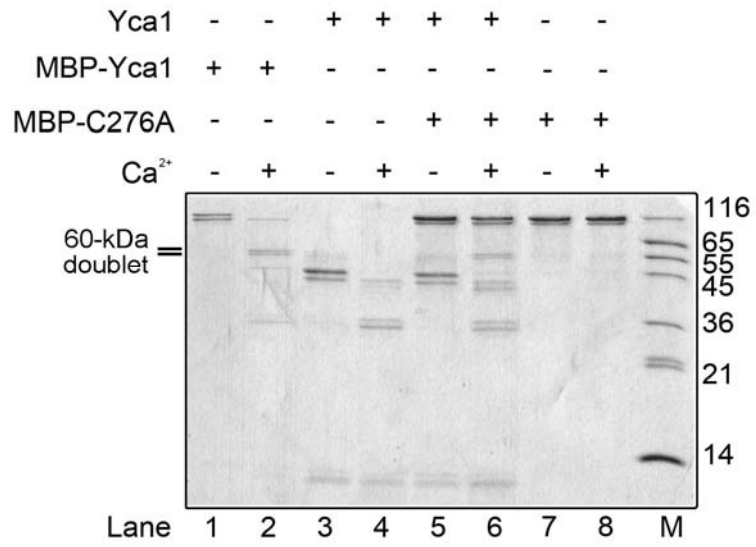
Supplementary Figure 4



Supplementary Figure 5



Supplementary Figure 6



References

1. Mittl, P. R., Di Marco, S., Krebs, J. F., Bai, X., Karanewsky, D. S., Priestle, J. P., Tomaselli, K. J., and Grutter, M. G. (1997) *J. Biol. Chem.* **272**, 6539-6547
2. Renatus, M., Stennicke, H. R., Scott, F. L., Liddington, R. C., and Salvesen, G. S. (2001) *Proc Natl Acad Sci* **98**(25), 14250–14255
3. Yu, J. W., Jeffrey, P. D., Ha, J. Y., Yang, X., and Shi, Y. (2011) *Proceedings of the National Academy of Sciences of the United States of America* **108**(52), 21004-21009
4. McLuskey, K., Rudolf, J., Proto, W. R., Isaacs, N. W., Coombs, G. H., Moss, C. X., and Mottram, J. C. (2012) *Proc Natl Acad Sci* **epub ahead of print**